

**"This is the peer reviewed version of the following article: FULL CITE, which has been published in final form at DOI: 10.1002/slct.201600242. This article may be used for non-commercial purposes in accordance With Wiley-VCH Terms and Conditions for self-archiving".**

## Amorphization of a Ru-Ru-Cd-Coordination-Polymer a Low Pressure

Franco Scalambra<sup>[a]</sup>, Manuel Serrano-Ruiz<sup>[a]</sup>, Dietrich Gudat<sup>[b]</sup>, Antonio Romerosa<sup>\*[a]</sup>

The water soluble backbone heterometallic polymer  $\{[(\text{PTA})_2\text{CpRu}-\mu\text{-CN-RuCp}(\text{PTA})_2-\mu\text{-CdCl}_3]\}_n$  (**1**), which is easily obtained in large amount, was synthesized and its structure determined by single crystal X-ray diffraction. Coordination-polymer **1** becomes amorphous when milled and under low pressure (0.5 MPa). The amorphous compound was characterized by MAS-NMR, elemental analysis, TG and Raman spectroscopy. The Raman spectrum of the coordination-polymer was assigned by comparison with the Raman spectrum obtained by DFT calculation of a simple model of **1**. The analysis of both calculated and experimental Raman spectra showed that Raman spectroscopy can be used to determine if the PTA ligand is mono- or bidentate, giving rise to a method for characterization and future studies of polymeric complexes containing bidentate PTA. The phase transformation of **1** under pressure and temperature was studied by PXR, showing how is possible to model easily this Ru-Ru-Cd inorganic polymer into a variety of different solid forms with possible new properties.

The synthesis of polyvinyl-ferrocenes<sup>[1]</sup> and metal-polyacetylides<sup>[2]</sup> started the design of new functional metal-containing polymers. The intense research focused on these new compounds led to the synthesis of promising materials useful in a variety of fields such as optical engineering, data storage, medicine, and catalysis.<sup>[3] [4] [5]</sup> Currently it is possible to build a variety of metal-containing supramolecular self-

assembled structure with outstanding and intriguing properties.<sup>[6]</sup> To date, very few examples of water-soluble coordination polymers including organometallic moieties are known, most of them based on 1,3,5-triaza-7-phosphaadamantane (PTA). This phosphine was known to act just as monodentate ligand until few years ago, but under adequate conditions, it is also a versatile polydentate building block suitable for the synthesis of hydrophilic metal-containing polymers and metal organic frameworks.<sup>[7]</sup> PTA is further well known as a useful ligand in complexes that are catalytically active in water or exhibit biological activity.<sup>[8]</sup> The first example of a water soluble organometallic polymer, the Ru-Ag heterometallic polymer  $\{[(\text{PTA})_2\text{CpRuDMSO}]-\mu\text{-AgCl}_2\}_n$ , was presented by our group in 2005, and the second one, the Ru-Ru-Au analogue  $\{[(\text{PTA})_2\text{CpRu}-\mu\text{-CN-RuCp}(\text{PTA})_2-\mu\text{-Au}(\text{CN})_4]\}_n$ , a few years later.<sup>[9]</sup> Both complexes maintain their polymeric structure in aqueous media, and the latter is the first example of an coordination-polymer with thermogel behaviour in water. In the last years, we have made an effort to find a systematic and reproducible method to obtain new heterometallic coordination-polymers containing the  $\{\text{CpRu}(\text{PTA})_2\}$  and  $\{\text{CpRu}(\text{PTA})_2-\mu\text{-CN-Ru}(\text{PTA})_2\text{Cp}\}$  units. The first success was the reproducible and robust synthesis of  $\{[(\text{PTA})_2\text{CpRu}-\mu\text{-CN-RuCp}(\text{PTA})_2-\mu\text{-NiCl}_3]\}_n$ ,<sup>[10]</sup> which displays also gel properties in water. Herein, we present a new example of this family of compounds, namely  $\{[(\text{PTA})_2\text{CpRu}-\mu\text{-CN-RuCp}(\text{PTA})_2-\mu\text{-CdCl}_3]\}_n$  (**1**).

The coordination-polymer **1** was obtained (experimental part in SI) by reaction of  $[(\text{PTA})_2\text{CpRu}-\mu\text{-CN-RuCp}(\text{PTA})_2]\text{OTf}^{[11]}$  with  $\text{CdCl}_2$  and further recrystallization in DMSO at 70 °C (Scheme 1). The synthetic procedure permits to obtain several tenths of grams of **1** in just one batch. The compound **1** is moderately soluble in water (14 mg/mL) and DMSO (8.1 mg/mL) and stable in both solvents at room temperature for weeks under air, but it is insoluble in MeOH, acetone, chloroform and toluene.

The crystal structure showed that **1** exhibits a 1D-backbone-consisting of dimeric ruthenium units  $\{(\text{PTA})_2\text{CpRu}-\mu\text{-CN-RuCp}(\text{PTA})_2\}^+$  and  $\{\text{CdCl}_3\}^-$  moieties which are

[a] F. Scalambra, Dr. M. Serrano-Ruiz, Prof. A. Romerosa  
Departamento de Química y Física-CIESOL  
Universidad de Almería  
04120, Almería, Spain  
E-mail: romerosa@ual.es

[b] Prof. D. Gudat  
Institut für Anorganische Chemie  
Universität Stuttgart  
Pfaffenwaldring 55, Stuttgart, Germany

Supporting information for this article is available on the WWW under <http://...>. Protocols, characterization data, accompanying spectra and PXRD diffractograms are provided for compound **1**.

coordinated to one N atom of two different PTA ligands situated at opposite sides of the Ru-CN-Ru axis. The cell contains also two DMSO molecules per repeating unit. Crystallographic parameters as well as selected bond lengths and angles are provided in Table S1, S2 and S3 in the SI.

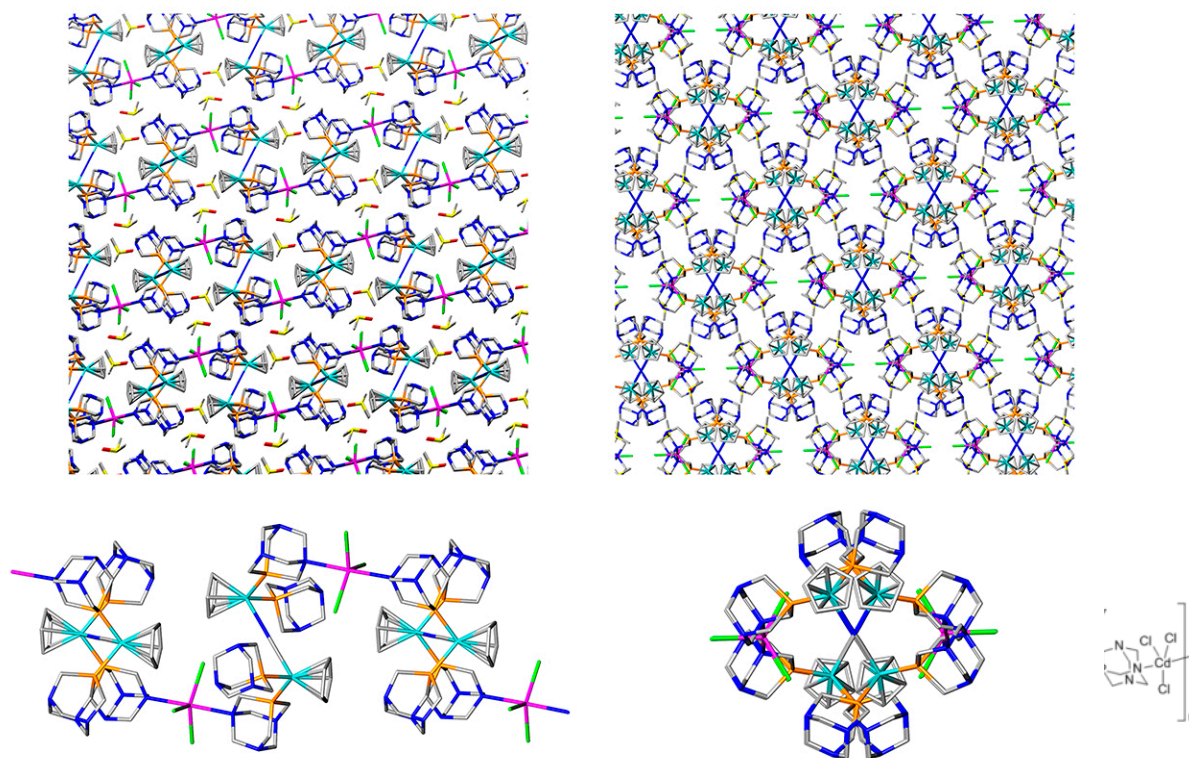
The  $\{\text{CpRu}(\text{PTA})_2\}^+$  moieties in each  $\text{Ru}_2$ -unit exhibit a transoid arrangement with respect to the Ru-CN-Ru axis. The CN bringing ligand is disordered (CN: 0.37(5)%; NC: = 0.63(5) %). The distances in the Ru-CN-Ru unit ( $\text{Ru1-C1C(N1C)} = 2.032(5) \text{ \AA}$ ;  $\text{Ru2-C1C(N1C)} = 2.032(5) \text{ \AA}$ ;  $\text{N1C}\equiv\text{C1C} = 1.158(7) \text{ \AA}$ ) are similar to those found in  $[(\text{PTA})_2\text{CpRu}-\mu\text{-CN}-\text{RuCp}(\text{PTA})_2]\text{OTf}$  ( $\text{Ru}-\text{CN}(\text{NC}) = 2.017(5) \text{ \AA}$ ;  $\text{C}\equiv\text{N} = 1.145(10) \text{ \AA}$ ),<sup>[4]</sup> which are also similar to those of Cp-ruthenium complexes containing bridging cyanide and more significantly of the polymers  $\{[(\text{PTA})_2\text{CpRu}-\mu\text{-CN}-\text{RuCp}(\text{PTA})_2]-\mu\text{-Au}(\text{CN})_4\}_n$  and  $\{[(\text{PTA})_2\text{CpRu}-\mu\text{-CN}-\text{RuCp}(\text{PTA})_2]-\mu\text{-NiCl}_3\}_n$ .<sup>[9,10]</sup>

The trigonal-bipyramidal Cd(II) is coordinated to three Cl in the equatorial and to two  $\text{N}_{\text{PTA}}$  atoms in the apical positions. The two  $\text{N}_{\text{PTA}}$  coordinated axially to the Cd are crystallographically equivalent ( $\text{Cd1-N11} = 2.438(3) \text{ \AA}$ ). The Cd coordination

geometry is somewhat distorted from an ideal trigonal-bipyramidal with two Cd-Cl bond lengths slightly different from the third one. The structural parameters are very similar to those of the complex (4-Aza-1-azoniabicyclo[2.2.2]octane)-(1,4-diazabicyclo[2.2.2]octane)-dichloro-cadmium,<sup>[12]</sup> which is the only other representative of a complex featuring a *tbp*-coordinated Cd-atom with three equatorial Cl and two axial N ligands found in the CSD data base.<sup>[13]</sup> There are no hydrogen bonds or other significant interactions among the coordination-polymer atoms and DMSO molecules, which are located in channels among the polymeric chains (Figure 2). Interestingly, the packing also displays further unoccupied channels (Figure 2).

Crystals of **1** become opaque after several hours of exposition to air. In view of the high boiling point of the included solvent, its evaporation is unlikely to be responsible for this effect. The X-ray powder diffraction from the opaque crystals is different than the calculated from the X-ray structure (Figure S8 SI) and therefore probably the polymer has been transformed at room temperature, suspecting by cleavage of the  $\text{N}_{\text{PTA}}\text{-Cd}$  bond.

**Figure 2.** Side and frontal views of the polymer chains and respective molecular packing to highlight the DMSO molecules disposition and the longitudinal holes between the channels



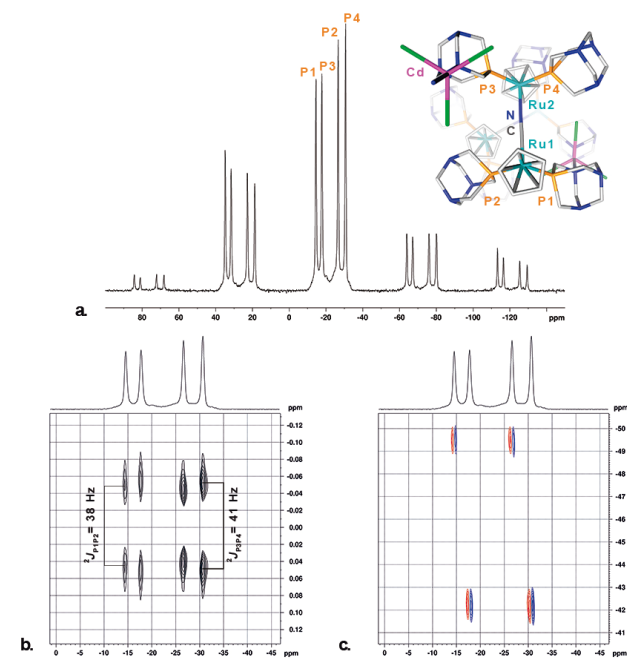


**Figure 3.**  $^{31}\text{P}$  CP-MAS NMR spectrum (a) and expansions of the  $^{31}\text{P}$ - $^{31}\text{P}$   $J$ -resolved spectrum (b) and  $^{31}\text{P}$  INADEQUATE spectrum (c) of **1**. The 2D spectra are expanded to display only the isotropic lines.

The CP-MAS NMR studies confirmed that the structural characteristics of crystalline **1** are conserved in the bulk sample. Figure 3 shows a  $^{31}\text{P}$  CP-MAS NMR spectrum, a  $^{31}\text{P}$ - $^{31}\text{P}$   $J$ -resolved spectrum, and a  $^{31}\text{P}$  INADEQUATE spectrum of **1**. The isotropic region of the  $^{31}\text{P}$  CP-MAS NMR spectrum shows two groups of two spinning sideband manifolds each centred at -14.5 ppm, -17.7 ppm and -26.6 ppm and -30.6 ppm, respectively. The INADEQUATE and  $J$ -resolved spectra reveal that the deshielded and the shielded signals in each group are connected by couplings of 39 Hz and 41 Hz which are of similar magnitude as previously observed  $^2J_{\text{PP}}$  coupling constants in Ru-PTA complexes,<sup>[14]</sup> indicating attachment of the appropriate phosphorus atoms to the same Ru atom. The observation of two signals in the  $^{31}\text{P}\{^1\text{H}\}$  NMR spectrum of  $[(\text{PTA})_2\text{CpRu}-\mu\text{-CN}-\text{RuCp}(\text{PTA})_2]^+$  in  $\text{D}_2\text{O}$  for the Ru-NC and Ru-CN bound PTA ligands (at -19.4 and -22.0 ppm) suggests that a similar deviation should also be expected for **1**. Additionally, alkylation or protonation of a coordinated PTA ligand induces a downfield shift of the  $^{31}\text{P}$  NMR signal in solution by some 12 ppm.<sup>[14]</sup> Based on these findings, we assign the peaks at -14.5 ppm to Cd-PTA-Ru-NC, -17.7 ppm to Cd-PTA-Ru-CN, -26.6 ppm to PTA-Ru-NC and that at -30.6 ppm to PTA-Ru-CN. The  $^{13}\text{C}$  CP-MAS experiments (Figure S4) show the methylene and Cp signals in the expected range (50-80 ppm). The signal of the cyanide carbon was identified by additional CPPI and NQS experiments with extended measuring time and different spinning rates as a broadened line at 151.9 ppm. The CPPI measurements helped also to characterize the PTA-methylene groups as the reduction in signal intensity is less pronounced in the less mobile bidentate than in the terminal ligand (Figure S4c).

Additional information was gained through Raman spectroscopy which is being successfully used for the

characterization of various metal-containing polymers and PTA-complexes.<sup>[15]</sup> To the best of our knowledge, there are no Raman spectroscopy studies on a system containing bidentate PTA. Whereas the infrared spectrum of these systems is dominated by strong, broad C-N absorptions which are hardly separable from the other key signals, the Raman spectrum of **1** shows a much clearer output. The interpretation of the spectrum was possible by a DFT evaluation of a model of the polymer structure as made in previous works.<sup>[16, 6a, 6c]</sup> A complete characterization of the vibrations of **1** can be found in the Supplementary Information (Table S3). The Terahertz region of the Raman spectrum of **1** is mainly constituted by the translational modes of the PTA ligands. Even if the spectral resolution is not enough to fully discriminate all the vibrations, one can distinguish at  $153\text{ cm}^{-1}$  the PTA torsions around the P-N-N-N centroid. This band is blue shifted ( $12\text{ cm}^{-1}$ ) with respect to that observed for  $[(\text{PTA})_2\text{CpRu}-\mu\text{-CN}-\text{RuCp}(\text{PTA})_2]\text{OTf}$ . The breathing vibrations in bidentate-PTA should split the signals to both up- and downfield with respect to the monodentate PTA, merely as a consequence of the reduction of the symmetry produced by coordination of the  $\text{N}_{\text{PTA}}$  to the Cd. This effect is evident in the split of the band at  $656\text{ cm}^{-1}$  found in  $[(\text{PTA})_2\text{CpRu}-\mu\text{-CN}-\text{RuCp}(\text{PTA})_2]\text{OTf}$ , which corresponds to a breathing motion localized in the upper rim (P-CH<sub>2</sub>-N) of the PTA (Supporting Information Figure S7) that is generated by P-C symmetric stretches. In **1** the bidentate PTA vibration arises at  $671\text{ cm}^{-1}$  and the band for monodentate PTA at  $654\text{ cm}^{-1}$ . The same trend is followed by the bottom rim (N-CH<sub>2</sub>-N) breathing motions centred at  $583\text{ cm}^{-1}$  in  $[(\text{PTA})_2\text{CpRu}-\mu\text{-CN}-\text{RuCp}(\text{PTA})_2]\text{OTf}$ , which arises for **1** at  $586\text{ cm}^{-1}$ . Unfortunately, these vibrations overlap strongly with some of cyclopentadienyl ring deformation modes. The CN stretching band is found at  $2109\text{ cm}^{-1}$ , as expected for a Ru(II)-Ru(II) bridging cyanide<sup>[17]</sup> while the weak broad shoulder at  $2816\text{ cm}^{-1}$  is assigned to the DMSO solvate.<sup>[18]</sup> These results show that Raman spectroscopy can be used to determine if the PTA ligand is mono- or bidentate, facilitating a method for future studies of metal-polymeric complexes containing PTA.

The crystallinity of the polymer depends on the powder particle size (Figure 4a): as soon as the particle size gets smaller the crystalline character of the polymer is reduced and polymer **1** becomes amorphous under  $75\text{ }\mu\text{m}$ . This fact made us consider the pressure imposed during powdering of the crystals as responsible for a structural transformation. Crystals of **1** became amorphous after just 15 minutes under 0.5 MPa argon pressure at room temperature. At such conditions, just a glassy band centred at  $2\theta = 34^\circ$  was observed (Figure 4, b, cyan). It is important to point out that to the best of our knowledge there are not examples of amorphization induced by so low pressure.<sup>[19]</sup> Pressure induced phase transformations in mixed inorganic-organic systems have been established just a few years ago and no such cases are reported for 1D-heterometallic polymers.<sup>[20]</sup> Higher pressure was applied to crystals of **1** by an IR press. At 1 GPa, formation of a new partially amorphous phase was noticed, which changed with increasing pressure but remained partially crystalline also at 10 Gps. The elemental analysis of the samples revealed the absence of any significant change in the composition and Raman spectroscopy supported that the  $\text{N}_{\text{PTA}}$ -Cd bond remained unaltered.

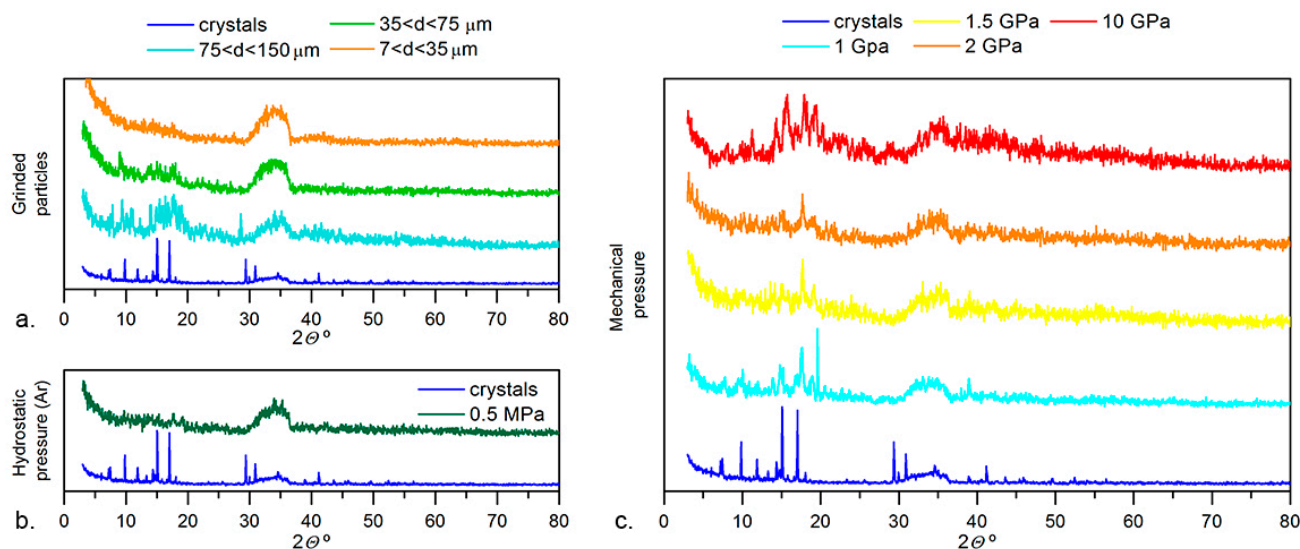


Figure 4. Amorphization and lattice transitions of **1**: PXRD of milled fractions (a); PXRD after exposition at increasing hydrostatic (b) and mechanical pressure (c).

To determine whether similar phase-transitions may be induced by temperature variation, the thermal behaviour of **1** was investigated. The thermogravimetric analysis of **1**, both crystalline and opaque, showed that the DMSO molecules were eliminated in two steps: at 158 °C, weight loss ascribable to one DMSO was observed, while the second molecule was removed at 196 °C. The PXRDs obtained at room temperature, 65 °C, 170 °C and 225 °C (Figure S9 SI) indicate that the structure of **1** changes with temperature. The PXRD shows as the crystalline phase of **1** changed at 65 °C in spite of DMSO molecules are not removed yet. Nevertheless, the most dramatic changes are observed when the first DMSO molecule was lost. At 170 °C, the PXRD revealed that the new phase is constituted by a significant glassy diffraction centred at  $2\theta = 34^\circ$ , independently of heating time. At 225 °C, a new crystalline phase was formed characterized by a small glassy diffraction similarly in intensity to that observed at room temperature. The TGA of a powdered sample that had first been heated to 225 °C and was then kept in air at room temperature for 2 h showed a weight loss at ca. 105 °C corresponding to five water molecules and no DMSO molecules elimination was observed. Several cycles of heating to 225 °C, cooling to ambient temperature, and subsequent analysis by TGA showed that the solid sample is able to loose and reincorporate water molecules without significant decomposition. Therefore, **1** is characterized by a non-common crystal-plasticity that produces amorphization under very low pressure and could provide opened structures by elimination of the DMSO solvent molecules.

Depending on the heating/pressurization rate, the amorphous materials thus formed can retain some aspects of crystalline topology, and consequently possess a lower configurational entropy than true glasses as observed for zeolites.<sup>[21]</sup> Comparisons between amorphization and melting conditions of inorganic polymers may provide further routes to more functional 'perfect' glasses, high-density amorphous (HDA)

inorganic glasses and melt-quenched hybrid glass (MQG). Furthermore, the back-bone inorganic polymer described here opens up possibilities for liquid casting and shaping heterometal inorganic polymers into a variety of different solid forms, promising to be an extremely exciting step forward in producing chemically functionalizable hybrid glass materials. The characterization of the structures derived from **1** under pressure and temperature are in progress as well as the study of their possible properties such as sensors and tuneable by pressure absorbent.<sup>[22]</sup>

## Acknowledgements

Thanks are given to the European Commission FEDER program for cofinancing the projects CTQ2015-67384-R (Ministerio de Economía y Competitividad, Spanish Government) and P09-FQM-5402 (Agencia de Innovación y Desarrollo de Andalucía, Junta de Andalucía). Thanks are also given to Junta de Andalucía PAI-research group FQM-317 and COST Action CM1302 (WG1, WG2). M. S-R. is grateful to Excellence project P09-FQM-5402 for a postdoctoral contract and F. S. to University of Almeria for a predoctoral grant.

**Keywords:** organometallic polymer; ruthenium; cadmium; amorphization; hybrid glass materials

- [1] F. S. Arimoto, A. C. J. Haven, *J. Am. Chem. Soc.* **1955**, *77*, 6295-6297
- [2] K. Sonogashira, S. Takahashi, N. Hagihara *Macromolecules* **1977**, *10*, 879-880
- [3] a) P. Nguyen, P. Gómez-Elípe, I. Manners, *Chem. Rev.* **1999**, *99*, 1515-1548; b) A.S. Abd-El-Aziz, C.E. Carraher, C.U. Pittman, M. Zeldin, *Inorganic and Organometallic Macromolecules*, Springer, New York,

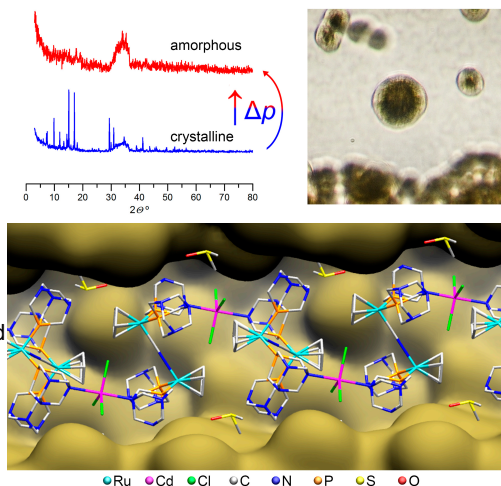
2008. c) M. Serrano-Ruiz, F. Scalambra, A. Romerosa in *Advances in Organometallic Chemistry and Catalysis: The Silver / Gold Jubilee International Conference on Organometallic Chemistry Celebratory Book*, (Ed.: A. J. L. Pombeiro), Wiley-VCH, Weinheim **2014**, pp 381-405; d) I. Manners, *Synthetic Metal-Containing Polymers*, Wiley VHC, Verlag GmbH & Co. KGaA, **2004**; e) U. S. Schubert, C. Eschbaumer, *Angew. Chem. Int. Ed.* **2002**, *41*, 2892-2926 f) G. R. Whittell, M. D. Hager, U. S. Schubert, I. Manners, *Nat. Mater.* **2011**, *10*, 176-188. g) Z. M. Hudson, D. J. Lunn, Winnik, A. Mitchell, I. Manners, *Nature Communications* **2014**, vol 5, article number: 3372.
- [4] T. Rudolph, A. Nunn, A. M. Schwenke, F. H. Schacher, *Polym. Chem.* **2015**, *6*, 1604-1612.
- [5] A. H. Shelton, R. S. Price, L. Brokmann, B. Dettlaff, K. S. Schanze, *ACS Appl. Mater. Interfaces*, **2013**, *5*, 7867-7874. b) X. Zeng, T. Zhang, Y. Qin, Z. Weia, M. Luo, *Dalton Trans.*, **2009**, 8341-8348
- [6] a) Z. M. Hudson, C. E. Boott, M. E. Robinson, P. A. Rupa, M. A. Winnik, I. Manners, *Nature Chemistry* **2014**, *6*, 893-898. b) T. Fukino, H. Joo, Y. Hisada, M. Obana, H. Yamagishi, T. Hikima, M. Takata, N. Fujita, T. Aida, *Science* **2014**, *344*, 499-504.
- [7] S. W. Jaros, M. F. C. Guedes da Silva, M. Florek, M. C. Oliveira, P. Smoleński, A. J. L. Pombeiro, A. M. Kirillov, *Cryst. Growth Des.* **2014**, *14*, 5408-5417.
- [8] a) M. Serrano-Ruiz, P. Lorenzo-Luis, A. Romerosa and A. Mena-Cruz, *Dalton Trans.* **2013**, *42*, 7622-7630. b) P. Smoleński, S. W. Jaros, C. Pettinari, G. Lupidi, L. Quassinti, M. Bramucci, L. A. Vitali, D. Petrelli, A. Kochel, A. M. Kirillov, *Dalton Trans.*, **2013**, *42*, 6572-6581. c) V. Ferretti, M. Fogagnolo, A. Marchi, L. Marvelli, F. Sforza, P. Bergamini, *Inorg. Chem.* **2014**, *53*, 4881-4890. d) A. D. Phillips, L. Gonsalvi, A. Romerosa, F. Vizza, M. Peruzzini, *Coord Chem Rev* **2004**, *11-12*, 955-993.
- [9] a) C. Lidrissi, A. Romerosa, M. Saoud, M. Serrano-Ruiz, L. Gonsalvi, M. Peruzzini, *Angew. Chem. Int. Ed.* **2005**, *44*, 2568-2572. b) M. Serrano-Ruiz, A. Romerosa, B. Sierra-Martin, A. Fernandez-Barbero, *Angew. Chem. Int. Ed.* **2008**, *47*, 8665-8669.
- [10] F. Scalambra, M. Serrano-Ruiz, A. Romerosa, *Macromol. Rapid Commun.* **2015**, *36*, 689-693.
- [11] M. Serrano-Ruiz, S. Imberti, L. Bernasconi, N. Jadagayeva, F. Scalambra, A. Romerosa, *Chem. Commun.* **2014**, *50*, 11587-11590.
- [12] Y. P. Huang, X. Zhang, L. Liu, N. X. Zhang, X. Z. Xu, W. H. Xuebao *Chin. J. Inorg. Chem.* **2014**, *30*, 1001-1008.
- [13] F. H. Allen, *Acta Cryst.* **2002**, *B58*, 380-388.
- [14] M. Serrano-Ruiz, P. Lorenzo-Luis, A. Romerosa, A. Mena-Cruz, *Dalton Trans.* **2013**, *42*, 7622-7630.
- [14] M. Serrano-Ruiz, L. M. Aguilera-Sáez, P. Lorenzo-Luis, J. M. Padrón, A. Romerosa, *Dalton Trans.*, **2013**, *42*, 11212-11219.
- [15] a) Adam M. Hawkridge and Jeanne E. Pemberton, *J. Am. Chem. Soc.*, **2003**, *125*, 624-625. b) J. Stezowski, E. Fluckbc, J. Weidlein, *Phosphorous and Sulfur and the Related Elements Vol. 4* **1978**, *2*, 199-204. c) S. W. Jaros, P. Smoleński, M. F. C. Guedes da Silva, M. Florek, J. Król, Z. Staroniewicz, A. J. L. Pombeiro, A. M. Kirillov, *CrystEngComm*, **2013**, *15*, 8060-8064.
- [16] a) K. Nakamoto in *Infrared and Raman Spectra of Inorganic and Coordination Compounds*, 5th edn, Wiley, New York, **1997**. b) R. M. Barr, M. Goldstein, *J. Chem. Soc., Dalton Trans.* **1974**, *11*, 1180-1185.
- [17] a) C. A. Bignozzi, R. Argazzi, J. R. Schoonover, K. C. Gordon, R. B. Dyer, F. Scandola, *Inorg. Chem.* **1992**, *31*, 5260-526. b) M. A. Watzky, J. F. Endicott, X. Song, Y. Lei, A. Macatangay, *Inorg. Chem.* **1996**, *35*, 3463-3473
- [18] Wayne N. Martens, R. L. Frost, J. Kristof, J. T. Klopogge, J. Raman Spectrosc. **2002**, *33*, 84-91
- [19] a) W. Cai, A. Gladysiak, M. Aniola, V. J. Smith, L. J. Barbour, A. Katrusiak, *J. Am. Chem. Soc.*, *137*, 9296-9301. b) D. Pinkowicz, M. Rams, M. Mišek, K. V. Kamenev, H. Tomkowiak, A. Katrusiak, B. Sieklucka, *J. Am. Chem. Soc.*, **2015**, *137*, 8795-8802. c) E. C. Spencer, M. S. R. N. Kiran, W. Li, U. Ramamurty, N. L. Ross, A. K. Cheetham, *Angew. Chem. Int. Ed.*, **2014**, *53*, 5583-5586. d) A. Prescimone, C. Morien, D. Allan, J. A. Schlueter, S. W. Tozer, J. L. Manson, S. Parsons, E. K. Brechin, S. Hill, *Angew. Chem.*, **2012**, *124*, 7490-7494. e) J. C. Tan, A. K. Cheetham, *Chem. Soc. Rev.*, **2011**, *40*, 1059-1080.
- [20] a) François-Xavier Coudert, *Chem. Mater.* **2015**, *27*, 1905-1916. b) G. N. Greaves, F. Meneau, O. Majerus, D. G. Jones, J. Taylor, *Science*, **2005**, *308*, 1299-1302. c) G. N. Greaves, F. Meneau, A. Sapelkin, L. M. Colyer, I. ap Gwynn, S. Wade and G. Sankar, *Nat. Mater.*, **2003**, *2*, 622-629.
- [22] J. R. Thompson, M. J. Katz, V. E. Williams, D. B. Leznoff, *Inorg. Chem.*, **2015**, *54*, 6462-6471.

Entry for the Table of Contents (Please choose one layout)

Layout 1:

## COMMUNICATION

The new water soluble backbone heterometallic coordination polymer  $\{[(\text{PTA})_2\text{CpRu}-\mu\text{-CN-RuCp}(\text{PTA})_2-\mu\text{-CdCl}_3]\}_n$ , was synthesized by a reproducible large scale method. Its structure was determined by single crystal X-ray diffraction. The crystalline sample amorphize when milled and under low pressure (0.5 MPa), opening up possibilities for shaping the heterometal inorganic polymer into a variety of different solid forms with possible new properties.



Franco Scalambra, Manuel Serrano-Ruiz, Dietrich Gudat, Antonio Romerosa\*

Page No. – Page No.

**Amorphization of a Ru-Ru-Cd-Coordination-Polymer a Low Pressure**